

The Role of Chlorine in the Regeneration by Hydrogen of Coked Reforming Catalysts

A. PARMALIANA,* F. FRUSTERI,* A. MEZZAPICA,† AND N. GIORDANO†

**Istituto di Chimica Industriale, Università di Messina, Via dei Verdi, 98100 Messina, Italy; and †Istituto CNR-TAE, Salita S. Lucia sopra Contesse 39, 98013 Pistunina Messina, Italy*

Received May 16, 1986; revised October 19, 1987

The effect of surface chlorine on the regeneration of several coked Pt/ γ -Al₂O₃ honeycomb reforming catalysts has been investigated. Catalytic activity in the dehydrogenation of methylcyclohexane (MCH) and regeneration tests at 400°C have been evaluated in a continuous flow micro-reactor. The determining role of surface chlorine is discussed and its optimum value has been established. A catalyst with ca. 0.5% Cl shows complete regeneration during static and dynamic hydrogen treatments. This behavior is attributed to a maximum in the hydrogen spillover from Pt to alumina, which restores the catalyst surface, freeing it of hydrocarbon residues. A mechanism for catalyst deactivation and regeneration is proposed. © 1988 Academic Press, Inc.

INTRODUCTION

Coke formation is the main cause of deactivation of bifunctional reforming catalysts. The economy of the petroleum refining and naphtha reforming operation, i.e., the need to increase the octane number, depends on the rate of catalyst deactivation. In spite of the practical importance of this phenomenon ("coking") and notwithstanding the fact that it has been the subject of intensive research for several decades, the formation and structure of the carbonaceous deposits on mono- or multimetallic reforming catalysts are still not well understood. A large number of papers (1–11) and several reviews (12–15) dealing with different aspects of coking have appeared.

The rate of deactivation of the catalyst depends mainly on the reaction temperature and partial pressure of hydrogen, but it is remarkable that the presence of hydrogen in the feed is not sufficient to avoid deactivation (coke formation) (4). Formation of unsaturated intermediates, which can condense or polymerize leading to coke, can be impeded by hydrogen through either a spillover (1, 5, 6) or a dynamic mechanism (9). Davis *et al.* (10) reported that the carbon

deposit during reforming on platinum single-crystal catalysts resulted from the activated nucleation and growth of unreactive polymeric species with an average hydrogen content of about 1.0–1.5 H atoms per surface C atom. Recently, it has been demonstrated that highly dispersed reforming catalysts are more resistant to deactivation from coke deposition (11). Parera and co-workers (6, 7) studied the influence of the chlorine content on deactivation of Pt/Al₂O₃ by coking and claimed that there is an optimum chlorine content which allows reduction of the coke deposit through a mechanism involving the activated spillover of hydrogen. Cooper and Trimm (3) claimed that the coking can be connected with the catalyst acidity related to the presence of Cl.

Generally, catalyst regeneration is achieved by heating in an oxidizing atmosphere (16, 17). This procedure may lead to further agglomeration of the metal and in some alloy catalysts it may alter the surface composition of metal particles or cause phase separation (18). In previous work we have reported that coked reforming catalyst can be "fully" restored by a nonoxidizing H₂ treatment at 400°C (19). The main goal

of the present study was to gain further insight into the effect of the surface acidity and surface chlorine content on the regeneration by hydrogen of coked reforming catalysts.

EXPERIMENTAL

Catalysts

Supported platinum catalysts were prepared from a ceramic honeycomb support of cordierite coated with a colloidal solution of $\gamma\text{-Al}_2\text{O}_3$ (Dispural Product, Condea, Hamburg) as described elsewhere (20). In order to differentiate between the influence of the surface acidity of $\gamma\text{-Al}_2\text{O}_3$ and the chlorine content in the catalyst regeneration, three series of catalysts were prepared: Ser.B, Ser.P, Ser.C. All catalysts were obtained by wet impregnation using a recirculation system. The catalysts of Ser.B were prepared by impregnation of the support with an ammoniacal solution of $\text{H}_2\text{Pt}(\text{OH})_6$ at different impregnation times. Catalysts of Ser.P were prepared by making use of a support previously doped with 1.5% P to depress the surface acidity of $\gamma\text{-Al}_2\text{O}_3$ (21). Afterward the P/ $\gamma\text{-Al}_2\text{O}_3$ honeycomb support was impregnated with the ammoniacal solution of $\text{H}_2\text{Pt}(\text{OH})_6$ at different impregnation times. The catalysts of Ser.C were prepared by impregnation with a H_2PtCl_6 solution with or without HCl (cats. C-2 and C-1, respectively). The catalysts were dried at 110°C for 24 h and then calcined in air at 500°C for 10 h. Catalysts C-1A and C-1B were obtained from cat. C-1 by dechlorination, based upon steam treatment at 500°C for 15 and 40 h, respectively (22). Results are compared with a previously (19) investigated commercial 0.24% Pt/ $\gamma\text{-Al}_2\text{O}_3$ honeycomb catalyst (PZM 4104, UOP, Des Plaines); the "as received" catalyst (here termed Z) was further subjected to dechlorination for 40 h (catalyst Z-B).

Catalysts Characterization

The Pt and P contents of the catalysts were determined photocolorimetrically using the stannous chloride and ascorbic acid

methods, respectively. The total amount of chlorine was determined by dissolution of the catalyst with sulfuric acid and titration of the distillate according to the Volhard-Charpenter method (7). It has been verified that the chlorine content of fresh and used catalysts does not change. Platinum particle size was determined by electron microscopy (JEOL 100 CX TEM instrument, point-to-point resolution 5 Å) using a finely ground and ultrasonically dispersed (in ethanol) catalyst sample, deposited on a thin carbon film supported on a standard copper grid.

The main physical and chemical characteristics of the catalysts used are given in Table 1.

Apparatus and Reaction Methods

Catalytic tests for the determination of the activity, stability, and regenerability of the catalysts were carried out in a continuous flow fixed-bed microreactor ($l = 200$ mm; i.d. = 14 mm) operating at atmospheric pressure. The hydrogen (PPL grade, SIO product) carrier gas, used also to prevent catalysts from deep deactivation, was purged by passing it through an O_2 trap (Alltech product), kept at room temperature (r.t.), followed by dehydration at r.t. in an "on-line" 13X molecular sieve bed. The purified hydrogen, regulated through a rotameter, was bubbled into a thermostatically controlled ($T = \pm 0.01^\circ\text{C}$) MCH saturator. MCH was RPE grade (Carlo Erba Product, purity $\geq 99.5\%$). The reaction mixture (H_2 saturated with MCH) was fed into the reactor containing the catalyst (0.1 g; 40–70 mesh). The catalyst was diluted with carborundum (1/30 vol/vol) to ensure quasi-ideal conditions for mass and heat transfer. Prior to reaction, the fresh catalysts were treated in hydrogen flow at 400°C for 2 h. Reactant and reaction products were analyzed by an on-line DANI 1800 gas chromatograph equipped with a TCD detector and a Spectra-Physics 3600 data processor.

RESULTS

MCH dehydrogenation was taken as a reaction model to study the deactivation process of the bifunctional reforming catalysts. Attempts were made to understand the regeneration of catalysts by the H₂ treatment, according to the static and dynamic methods described below.

MCH Dehydrogenation Catalytic Test

All catalysts were tested at 400°C and WHSV = 48 h⁻¹. Runs were carried out at atmospheric pressure and with a molar ratio $R = P_{H_2}/P_{MCH}$ of 2. Helium (350 cm³ STP min⁻¹) was used as a carrier and N₂ (10 cm³ STP min⁻¹) as an internal standard. On account of this, the molar ratio $R' = (P_{H_2} + P_{N_2} + P_{He})/P_{MCH}$ was 20. The performance of the catalysts was recorded during a period of 6 h. As no other product besides toluene was observed, the conversion to toluene was taken as a measure of the catalytic activity. The values of initial and final activity for all catalysts are summarized in Table 2.

Catalyst Regeneration Test

H₂ static method. After a 6-h run at $T = 400^\circ\text{C}$ the reaction mixture was vented and the "coked" catalyst was treated by a 500 cm³ STP min⁻¹ He flow for 10 min. Then the catalyst was kept at 400°C in a He static atmosphere for 14 h.

H₂ dynamic method. After a 6-h run at $T = 400^\circ\text{C}$ the reaction mixture was vented and the "coked" catalyst was treated by a 500 cm³ STP min⁻¹ H₂ flow for 6.5 h. During this regenerative process, the catalyst temperature was carefully monitored and found constant.

Products formed during the regeneration test by the H₂ static method have been analyzed by a gas chromatograph unit. On cats. C-1B and Z-B the presence of CH₄ and C₂H₆ has been revealed together with traces of C₂H₂. No such products were noted on the other catalysts.

After regeneration, each catalyst was

TABLE I
Catalyst Properties

Catalyst:	B-1	B-2	P-1	P-2	C-1	C-1A	C-1B	C-2	Z	Z-B
$\gamma\text{-Al}_2\text{O}_3/\text{honeycomb}$ (wt/wt)	0.15	0.15	0.15	0.15	0.15	0.15	0.15	0.15	n.d.	n.d.
BET surface area (m ² g ⁻¹)	27	27	23	23	27	27	27	27	28	28
Precursor of platinum	H ₂ Pt(OH) ₆	H ₂ Pt(OH) ₆	H ₂ Pt(OH) ₆	H ₂ Pt(OH) ₆	H ₂ PtCl ₆	H ₂ PtCl ₆	H ₂ PtCl ₆	H ₂ PtCl ₆	Unknown	Unknown
Pt content (wt%)	0.19	0.13	0.23	0.15	0.26	0.26	0.26	0.03	0.24	0.24
Cl content (wt%)	—	—	—	—	1.75	0.95	0.53	2.50	1.0	0.50
P content (wt%)	—	—	1.5	1.5	—	—	—	—	—	—
MSA (m ² Pt g ⁻¹ Pt)	233	233	310	310	350	200	140	n.d. ^b	56	53
Pt dispersion (%)	94	94	100	100	100	81	57	n.d.	23	21
Mean crystallite size (Å) ^a	12	12	9	9	8	14	20	n.d.	50	53

^a Measured by TEM analysis.

^b n.d., not determined.

TABLE 2
Catalytic Activity of Reforming Catalysts in MCH Dehydrogenation at 400°C

Cat.	Pt (wt.%)	Mean crystallite size (Å)	Initial activity (% MCH conv.)	Final activity (% MCH conv.)
B-1	0.19	12	52.2	15.4
B-2	0.13	12	38.5	21.4
P-1	0.23	9	56.4	20.2
P-2	0.15	9	40.0	13.2
C-1	0.26	8	50.0	15.8
C-2	0.03	n.d.	5.0	3.0
C-1A	0.26	14	35.0	10.8
C-1B	0.26	20	32.0	14.0
Z	0.24	50	27.0	12.0
Z-B	0.24	53	20.0	10.0

tested (with the same procedure as that for the initial run) in order to check the level of its initial activity restoration. Coked catalysts were subjected to both regeneration methods; the most significant experimental results of these regeneration tests are summarized in Table 3. The behavior of the catalysts of the three series and that of the commercial one was compared. It was found that only catalysts C-1B and Z-B could be regenerated by both methods, with no substantial differences in the efficiencies of regeneration. Furthermore, results collected in Table 3 show that in the case in which no total regeneration occurs (through the H₂ regeneration tests), restoration of

activity is a fraction of the original one. The behavior of some typical catalysts (cats. C-1 and C-1B) during a deactivation-H₂ regeneration cycle is shown in Fig. 1. It can be noted that for cat. C-1 the H₂ regeneration methods are not able to restore the initial activity of the catalyst, while cat. C-1B was regenerated by both the static and the dynamic H₂ treatments.

IR Analysis of Coke Deposits

IR spectra of the coked catalysts were obtained, after heating under vacuum at 125°C, using a UR-20 spectrometer within the range 1200–4000 cm⁻¹. The spectra revealed the following:

TABLE 3
Regeneration Tests of Coked Catalysts

Cat.	Cl (wt.%)	Initial activity (% MCH conv.)	Initial activity after regeneration test	
			H ₂ static method (% MCH conv.)	H ₂ dynamic method (% MCH conv.)
B-1	—	52.2	34.7	35.9
P-1	—	56.4	28.8	31.8
C-1	1.75	50.0	26.2	28.3
C-1A	0.95	35.0	20.4	20.5
C-1B	0.53	32.0	31.5	31.5
Z	1.0	27.0	18.3	18.8
Z-B	0.50	20.0	19.0	19.0

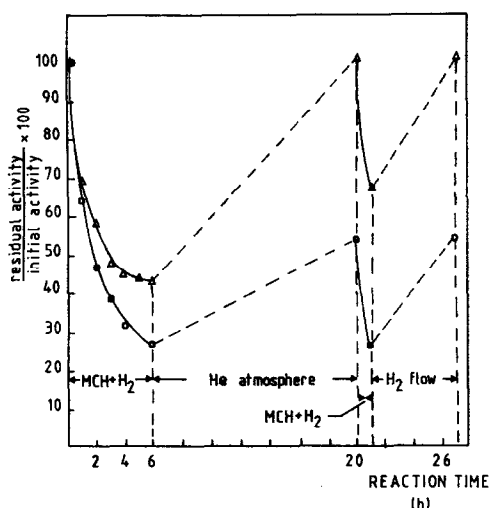


FIG. 1. Deactivation and subsequent regeneration tests of catalyst at 400°C, WHSV = 48 h⁻¹, $R = P_{H_2}/P_{MCH} = 2$ (Δ , cat. C-1B; \circ , cat. C-1).

(a) Four absorption bands at 1420–1470, 2860–2890, 2930–2940, 2960–2980 cm⁻¹ characterizing stretchings of CH bonds in CH₂ and CH₃ groups (13, 23);

(b) two absorption bands at 1490 and 1590 cm⁻¹ characterizing stretchings of aromatic rings (13, 23);

(c) one absorption band near 3020 cm⁻¹ attributable to the stretching of the C–H bond in unsaturated or aromatic compounds (13, 23).

It was noted that coke on catalysts C-1, C-1A, and C-1B had the same nature, attributable to (linear) saturated hydrocarbon compounds. On the contrary, on catalyst B-1, the coke was assignable mainly to aromatic compounds.

DISCUSSION

H₂ Regeneration of Coked Reforming Catalyst

It is well known that the presence of H₂ in the feed during reforming reduces the quantity of carbonaceous deposits (13). Moreover, it is generally agreed that H₂ exerts a hydrogenolytic activity on these deposits thus allowing their fast surface de-

sorption (1, 2, 6, 13). According to some authors the function of H₂ is to be attributed to spillover of molecular H₂, followed by hydrogenolytic activity of the so-formed atomic hydrogen (1, 5), and for which a determining role of surface Cl has been postulated by Parera *et al.* (5, 6). Our experimental results clearly indicate that as only catalysts C-1B and Z-B appear to be fully regenerable by H₂ treatment in the static and dynamic methods, the presence of chlorine is a prerequisite. Moreover, due to the equivalent results by the two methods, we suggest that the regeneration process by the “H₂ static method” must be related either to the residual H₂, formed ab initio (chemisorbed) on the surface during the catalytic reaction, or to that retained by the carbonaceous residues, well in agreement with their different reactivity, as claimed by Davis and co-workers (10). In the “H₂ dynamic method,” on the other hand, besides the above-hypothesized role of residual hydrogen, also the dynamic effect of flowing H₂ on coked catalysts contributes to achieve the catalyst regenerability in a shorter time, probably by determining the H₂ saturation of accessible catalytic surface.

As to the influence, if any, of particle size it has been reported in the literature that the number of carbon atoms deposited per platinum surface site increases with the platinum particle size (11). This leads to the assumption that the regenerability of larger platinum crystallites could be more difficult than that of the smaller ones. As our results reported in Table 3 show that catalyst C-1B, characterized by larger platinum crystallites than catalysts C-1 and C-1A, is fully regenerable, the influence of this parameter can be disregarded. In order to evaluate the influence of the nature of hydrocarbon residues in catalyst regenerability, it must be noted that IR analysis of coked catalysts revealed the coke on the C-1, C-1A, and C-1B samples to have the same nature, i.e., linear saturated hydrocarbon residues. Therefore the full regenerability of catalyst

C-1B cannot be attributed to more easily removable carbonaceous residues. This evidence indicates that the chlorine content constitutes the determining factor controlling the catalyst regenerability.

On the basis of the mechanism postulated before (19), we suggest an interpretation based upon dissociative H_2 chemisorption and subsequent migration by a spillover mechanism. Hydrogenolysis of the unsaturated carbonaceous residues is postulated to occur by means of atomic H, followed by desorption (as light hydrocarbons) which frees the active sites. The above is based upon the presence of CH_4 , C_2H_2 , C_2H_6 which are found exclusively in desorbed products from catalysts C-1B and Z-B. The mere observation that this occurs on samples containing ca. 0.5% Cl was taken as an indication that spillover activity, if any, must be related to the Cl content. This indeed also appears to be the case in the work of some authors who have found the spillover to be influenced by the Cl content of the catalyst (24, 25). Benke (24) suggested that the optimal concentration of Cl for the spillover on Al_2O_3 is on the order of 3×10^{13} atoms/cm² and that, at the higher Cl concentrations, the few Al ions left on the surface limit the proton migration because of the hindrance to the migration of hydride ions which are necessary to maintain electrical neutrality. On account of this hypothesis it is instructive to note that the number of OH groups on Al_2O_3 has been reported to be 20×10^{13} cm⁻² by Tanaka and Ogasawara (26) for the γ - Al_2O_3 heat-treated at 500°C and 20×10^{14} cm⁻² by Kramer and André (27) for samples heat-treated at 400°C. Recently, certain authors (28) have indicated a saturation value of the Cl atoms on γ - Al_2O_3 of 10×10^{13} atoms/cm² which is of the same order of magnitude as the number of OH groups. In consideration of the above, we assume that on those samples characterized by 0.5 wt% Cl content (cats. C-1B and Z-B), half of OH groups are replaced by Cl^- ions, and this gives rise to maximum spillover. Under such conditions

a quasi-neutrality in the surface electrical charges is assumed. In agreement with other authors (6, 24), we claim that this constitutes a fundamental factor for high spillover, probably through an ionic diffusion mechanism. The assumptions made above appear to justify the nonregenerability of samples C-1 (1.75% Cl), C-1A (0.95% Cl), and Z (1% Cl) with calculated values of 1.7×10^{14} , 8.5×10^{13} , and 9×10^{13} Cl atoms/cm², respectively. Such a high Cl coverage on the surface of these samples should prevent conditions of electrical neutrality and therefore impede high hydrogen spillover.

Reaction Mechanism for MCH Dehydrogenation and Coking

As claimed above, the optimum surface chlorine content (= 0.5%) plays an important role by favoring hydrogen spillover and dynamic hydrogenation of hydrocarbon residues. So far, little has been stated with respect to the influence of chlorine content on the nature and mechanisms of formation of carbonaceous residues contributing to coking and thus we lack a satisfactory answer to these questions. Our experimental findings, namely the identification of certain desorption products for cats. C-1B and Z-B, the different regenerability of the catalysts of the three series, and IR analysis of coked catalysts, lead us to propose the model for coking shown in Fig. 2. It lies upon the well-accepted assumption that MCH can chemisorb on the metallic site in two ways (3, 9, 10), namely by (a) active chemisorption (step I), which determines dehydrogenation to methylcyclohexene (MCH^{2-}) and finally toluene, and by (b) self-poisoning chemisorption (step II) which gives rise to the formation of partially unsaturated hydrocarbon residues (C_nH_m) on the catalyst surface and thereafter to the blocking of metallic sites (3, 10). As step II can be attributed to the higher chemisorption energies of some of the metallic sites, we assume that the self-poisoning chemisorption of the reactant (step II)

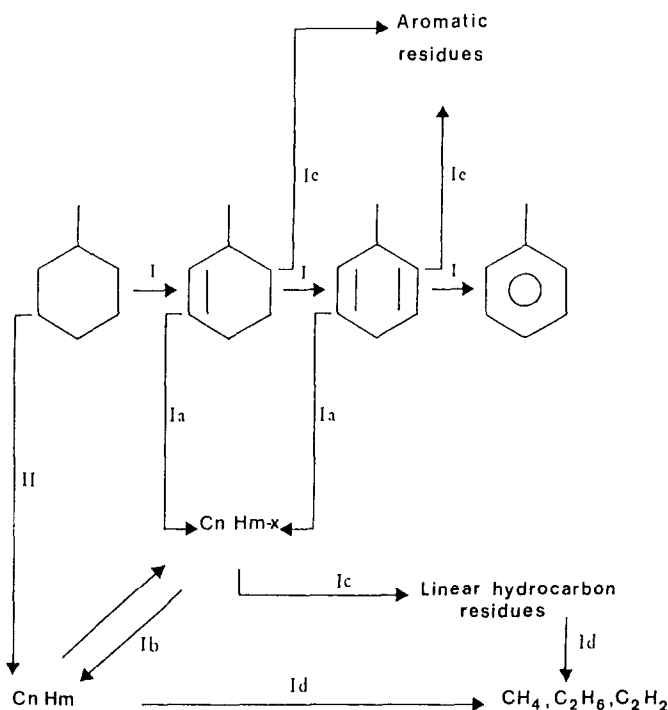


FIG. 2. Reaction mechanism for MCH dehydrogenation and coking on reforming catalyst.

contributes to deactivation of all catalysts in a similar manner, irrespective of surface acidity and Cl content. Evidently this is due to the fact that such residues originate on the metallic sites and participate as a nonselective poison; i.e., the residues block the platinum surface preventing chemisorption of the impinging reactant molecules (10). In considering the above, it should be taken into account that precursors such as MCH^{2-} and methylcyclohexadiene, which are more prone to cracking, probably contribute to coking but in a different manner depending on surface acidity (Cl), i.e., by a desorption process from the metallic sites and subsequent adsorption on the acidic sites with ring opening (step Ia). The hydrocarbon residues generated in the ring opening reaction (C_nH_{m-x}) can polymerize through an acid (Cl)-catalyzed process (step Ic) to form linear saturated hydrocarbon residues. For the chlorine-free catalysts the open ring reaction, occurring on

acid sites, is not relevant, while MCH^{2-} and methylcyclohexadiene can also react (step Ic) to form hydrocarbon residues having mainly an aromatic nature. IR analysis of coked catalysts confirms the above assumptions, revealing linear hydrocarbon residues on chlorided catalysts (series C) and hydrocarbon aromatic compounds on chlorine-free catalyst (cat. B-1).

We assume that eventually formed C_nH_{m-x} residues are in dynamic equilibrium with species C_nH_m (step Ib). This assumption is based on the observed positive influence exerted by H_2 , in accordance with the literature (6, 9, 10).

The linear saturated hydrocarbons and C_nH_m residues chemisorbed on the catalyst can be removed through a hydrogenolytic mechanism (step Id). The experimental verification of step Id, revealing the presence of CH_4 , C_2H_6 , and C_2H_2 in desorbed products for cats. C-1B and Z-B, confirms the above-proposed deactivation and regenera-

tion mechanism and the determining role of an optimum surface chlorine content (0.5% Cl) on the hydrogen spillover.

ACKNOWLEDGMENTS

The authors are grateful to Professor A. Iannibello for helpful discussions and Mr. F. Gulletta for experimental assistance. The financial support of this study by CNR is gratefully acknowledged.

REFERENCES

1. Shum, V. K., Butt, J. B., and Sachtler, W. M. H., *Appl. Catal.* **11**, 151 (1984).
2. Völter, J., and Kurschner, U., *Appl. Catal.* **8**, 171 (1983).
3. Cooper, B. J., and Trimm, D. L., in "Catalyst Deactivation" (B. Delmon and G. F. Froment, Eds.), p. 63. Elsevier, Amsterdam, 1980.
4. Jossens, L. W., and Petersen, E. E., *J. Catal.* **73**, 377 (1982).
5. Parera, J. M., Traffano, E. M., Musso, J. C., and Pieck, C. L., "Spillover of Adsorbed Species" (G. M. Pajonk, S. J. Teichner, and J. E. Germain, Eds.), p. 101. Elsevier, Amsterdam, 1983.
6. Parera, J. M., Figoli, N. S., Jablonski, E. L., Sad, M. R., and Beltramini, J. N., "Catalyst Deactivation" (B. Delmon and G. F. Froment, Eds.) p. 571. Elsevier, Amsterdam, 1980.
7. Figoli, N. S., Sad, M. R., Beltramini, J. N., Jablonski, E. L., and Parera, J. M., *Ind. Eng. Chem. Prod. Res. Dev.* **19**, 545 (1980).
8. Delannay, F., Defossé, C., Delmon, B., Menon, P. G., and Froment, G. F., *Ind. Eng. Chem. Prod. Res. Dev.* **19**, 537 (1980).
9. Coughlin, R. W., Kawakami, K., and Hasan, A., *J. Catal.* **88**, 150 (1984).
10. Davis, S. M., Zaera, F., and Somorjai, G. A., *J. Catal.* **77**, 439 (1982).
11. Barbier, J., Corro, G., Zhang, Y., Bournonville, J. B., and Franck, J. P., *Appl. Catal.* **13**, 245 (1985).
12. Trimm, D. L., *Appl. Catal.* **5**, 263 (1983).
13. Wolf, E. E., and Alfani, F., *Catal. Rev. Sci. Eng.* **24**, 329 (1982).
14. Froment, G. F., in "Catalyst Deactivation" (B. Delmon and G. F. Froment Eds.), p. 1. Elsevier, Amsterdam, 1980.
15. Butt, J. B., in "Catalyst Deactivation" (B. Delmon and G. F. Froment, Eds.), p. 21. Elsevier, Amsterdam, 1980.
16. Straguzzi, G. I., Aduriz, H. R., and Cigola, C. E., *J. Catal.* **66**, 171 (1980).
17. Bournonville, J. P., Franck, J. P., and Martino, G., in "Preparation of Catalysts III" (G. Poncelet, P. Grange, and P. A. Jacobs, Eds.), p. 81. Elsevier, Amsterdam, 1983.
18. Foger, K., and Jaeger, M., *J. Catal.* **92**, 64 (1985).
19. Frusteri, F., Barcellona, V., Mento, G., Parmaliana, A., and Giordano, N., *Ann. Chim. (Rome)* **75**, 441 (1985).
20. Giordano, N., Parmaliana, A., Frusteri, F., Mento, G., and Mezzapica, A., Italian Patent No. 48666A83 (1983).
21. Gishti, K., Iannibello, A., Marengo, S., Morelli, G., and Tittarelli, P., *Appl. Catal.* **12**, 381 (1984).
22. Castro, A. A., Scelza, O. A., Benvenuto, E. R., Baronetti, G. T., and Parera, J. M., *J. Catal.* **69**, 222 (1981).
23. L. J. Bellamy, "The Infrared Spectra of Complex Molecules," p. 13. Chapman & Hall, London, 1975.
24. Benke, A. H., Ph.D. thesis, University of California, Berkeley, 1976.
25. Bond, G. C., Fuller, J. M., and Molloy, L. R., "Proceedings, 6th International Congress on Catalysis, London, 1976" (G. C. Bond, P. B. Wells, and F. C. Tomkins, Eds.), p. 356. The Chemical Society, London, 1977.
26. Tanaka, M., and Ogasawara, S., *J. Catal.* **16**, 157 (1970).
27. Kramer, R., and André, M., *J. Catal.* **58**, 287 (1979).
28. Lietz, G., Lieske, H., Spindler, H., Hanke, W., and Völter, J., *J. Catal.* **81**, 17 (1983).